IEEE Access
Multidisciplinary ⋮ Rapid Review ⋮ Open Access Journal

Received January 22, 2022, accepted February 4, 2022, date of publication February 7, 2022, date of current version February 18, 2022.

Digital Object Identifier 10.1109/ACCESS.2022.3149802

Fuzzy Based Condition Monitoring Tool for Real-Time Analysis of Synthetic Ester Fluid as Transformer Insulant

MRIDULA, SHUFALI ASHRAF WANI, A. J. AMALANATHAN, AND R. SARATHI, (Senior Member, IEEE)
Department of Electrical Engineering, IIT Madras, Chennai 600036, India

Corresponding author: R. Sarathi (rsarathi@iitm.ac.in)

This work was supported by the Science and Engineering Research Board (SERB), New Delhi, India, under Grant CRG/2020/003525/EEC (for advanced transformer insulation).

ABSTRACT The main aim of the present study is to explore the use of synthetic ester fluid as a transformer insulant. For this, the performance of thermally aged synthetic ester is investigated using corona inception voltage (CIV) measurement, fluorescent analysis, and dielectric spectroscopic studies. Then a fuzzy model is introduced to correlate the outcome of these studies to predict the key performance index and lifetime estimation of insulation structures. CIV tests for the thermally aged ester fluid, under AC voltage show 53.2% and 34% reduction in inception values due to ageing time and ageing temperature respectively. Furthermore, the effect of magnetic field on the performance of thermally aged ester is also studied and a drastic reduction of 54.3% and 39.4% respectively in CIV is observed. Statistical studies also indicate accelerated degradation of the insulation performance under the influence of the magnetic field, showing high scatter in CIV data indicated by decreasing beta values. Other studies such as fluorescent spectroscopy depict progressive shifts in fluorescence maxima and a decrease in emission intensity with ageing. Dielectric spectroscopy results show a manifold increase in dissipation factor due to thermal ageing. A fuzzy monitoring tool uses spectral data as input and at the output indicates the level of deterioration. The Rule-base of the model is framed using dielectric study.

INDEX TERMS Ester, corona, magnetic field, frequency, hysteresis, Weibull, fluorescence, dielectric loss, fuzzy model.

I. INTRODUCTION

Transformers form an essential part of the power system network. The information about the longevity of transformers is determined basically by the health of their insulation. Mineral oil is the most commonly used insulating liquid used in transformers. However, moisture intolerance, non-biodegradability and corrosive nature due to sulphur formation provoke the search of finding better alternatives of existing mineral oil [1]–[5]. The new age insulating liquids viz., synthetic ester fluids are gaining popularity due to their high biodegradability, higher flash point, fire point and moisture tolerance. The increased moisture tolerance allows more water, resulting from cellulose to be absorbed by ester fluids. This results in slower ageing of solid insulation thereby enhancing the life of transformers [6], [7]. However, degradation of transformer insulation due to inevitable thermal ageing causes impairment of these properties and results in impending faults. Such faults if left unattended may lead to catastrophic failure of insulation structure and hence continuous assessment of insulation condition becomes essential. Since the condition of the oil is a direct indicator of transformer condition, therefore condition monitoring of transformers is majorly associated with the timely assessment of the condition of oil.

A widely used traditional technique for transformer condition monitoring is Dissolved Gas Analysis (DGA). However, it helps in incipient fault recognition and cannot assess the ageing condition of oil. Chemical tests for moisture and acidity calculation of oil are also helpful in predicting the health of aged oil but these are time-consuming [8]. One of the major problems in transformers is the discharge initiated

The associate editor coordinating the review of this manuscript and approving it for publication was Giovanni Pau.

from a weak link caused due to micro protrusion in the winding or edge of the winding, where the local electric field can enhance causing corona discharge activity. [9]. Therefore, analysis of corona discharge is an important study to investigate the condition of transformer oil [10]. The effect of thermal ageing on corona discharge activity in mineral oil and natural ester under different voltage profiles were studied [11]. Apart from the local electric field, the magnetic field within the transformers can also influence the partial discharge (PD) activity [12]–[14]. However, in literature, a study of magnetic field influence on PD characteristics variation is limited. Hence, analysis of corona discharge activity under the combined effect of ageing especially due to thermal effect and the magnetic field is an important research gap.

There are various established techniques for identification of corona discharge albeit condition monitoring of oil such as traditional PD studies, acoustic emission technique, ultra-high frequency (UHF) and non-destructive optical absorption and emission measurement techniques [15], [16]. To name a few, Ultra-violet (UV) spectrophotometry [17], Infrared (IR) spectroscopy [18], photoluminescence (PL) spectroscopy [19] and fluorescent spectra [20] are used to understand the characteristic variation in the composition of thermally aged oil and are a modern-day alternative to traditional condition monitoring. The optical measurement technique adopting fluorescent fibre for sensing PDs in liquid insulation is also gaining popularity but the technique is still in infancy [21]. Research shows that the information present in the spectral data can be extracted and different classification techniques are employed depending upon the type of application [22]. Artificial neural networks (ANN) and k-nearest neighbours (kNN) are also widely used for the classification of spectral data [23].

With the aim of automating the transformer condition monitoring practice and adjusting the uncertainties due to manual interface, artificial intelligence (AI) techniques are gaining popularity. AI-based condition monitoring and assessment systems are nowadays used to solve many practical transformer operation problems [24]. Hence the information obtained from these sensitive optical techniques can be precisely used to predict the health of transformer insulation using an AI-based model. Having known all these aspects, the following methodical experimental studies need to be carried out with thermally aged synthetic ester: (i) analysis of corona inception voltage (CIV) variation in presence of magnetic field under AC voltages ii) statistical analysis of CIV variation in presence of magnetic field (iii) fluorescent spectroscopy analysis and dissipation factor variation (iv) construction of a fuzzy model to correlate the performance analysis of thermally aged synthetic ester using these characterizations and to predict the status on the end life of the insulation.

II. EXPERIMENTAL PROCEDURE AND DISCUSSIONS

Synthetic ester fluid (Midel 7131) is used for studying the effect of thermal ageing and characteristic variation in its performance. Thermal ageing is carried out according to IEC 62332-2 [25]. Pressboard strips of dimension $4 \times 4 \times 0.2$ cm are dried at 90°C for 24 h and then wrapped in a thin copper sheet before immersing in oil samples. The weight ratio of fluid: pressboard: copper is maintained at 10:1:1. 100 ml test samples aged for different periods at fixed temperature and also at different temperatures for a fixed time are used for experimental purposes. Ageing is carried for 25 h, 50 h, 100 h, 300 h, 500 h and 1000 h in a thermally controlled oven at 160°C. Further, for the pre-fixed time of 250 h, ageing is also carried out at 120°C, 140° C, 160°C and 180°C. For reference purposes, unaged fluid with pressboard strips, preheated at 90°C for 24 h is also tested. The electrical characterization of the synthetic ester is carried out using the Corona Inception Voltage (CIV) test. The experimental set-up for generating corona type insulation defects includes (a) High voltage source (b) Test sample (c) Magnetic field source (d) Detection source e) High bandwidth digital storage oscilloscope (DSO). The high voltage input to the oil sample under test is obtained from the Trek amplifier (TREK-MODEL20/20C). The oil sample is placed in a test cell with a needle-plane electrode configuration for generating corona discharges. The diameter of the needle is 100 μm and that of the bottom plane is 5 cm. Fig. 1 shows the experimental set-up for the CIV test with an arrangement of the external magnetic field. The high voltage input is connected to the needle and the bottom plane is grounded. To prevent the breakdown of liquid especially at minimum needle-plane gap distance, respectively aged pressboard strips for different fluids are used as a barrier in between plane and needle. Besides the arrangement, two permanent magnets are used to analyse the variation in CIV due to an external magnetic field up to 160 mT.

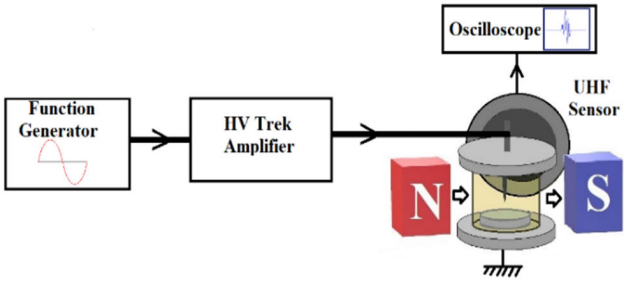

FIGURE 1. Experimental setup for corona inception voltage measurement.

UHF sensor is used for sensing the corona activity due to insulation defects. Corona activity results in the rupture of electrons from the atoms which get accelerated under the effect of the electric field and come to rest after some time. The acceleration of electrons causes electromagnetic radiations to occur. UHF sensor picks up these electromagnetic signals generated due to corona discharge and the corresponding electrical signal is displayed on 4 channel digital storage oscilloscope (Lecroy Model Wavepro). UHF sensor being highly sensitive is kept at a distance greater than 20 cm from the test cell (the source of PD).

A. ELECTRICAL CHARACTERIZATION

1) CIV TEST

To assess the insulating strength of synthetic ester, a CIV test is conducted. Corona insulation defect is created using needle-plane configuration and inception voltage of unaged and aged test samples is measured. The test is conducted under an AC voltage profile to analyze the combined effect of thermal ageing and magnetic field on CIV. The inception voltage for each sample is measured by varying the distance between the needle and the ground plate. A simultaneous magnetic field of 160 mT is introduced to observe its effect on corona inception at each gap distance. Fig. 2(a) and (b) shows the variation of CIV with thermal ageing due to fixed temperature (160°C) and fixed ageing time (250 h) respectively at different needle plane gap distances. CIV shows an inverse relationship with ageing duration in Fig. 2(a) and ageing temperature in Fig. 2(b). Due to thermal ageing, the insulating strength of fluid decreases and the inverse relationship of CIV and ageing time/temperature verifies that. Since the electric field required for the generation of corona discharges in synthetic ester is nearly constant and hence higher voltage is required to produce the same electric field when the distance between high voltage electrode and ground is increased [26]. It is found that ionization of liquid near the needle tip during negative cycle results in accumulation of charges and positive cycle prevents the build-up of charges and the resulting electric field initiates the discharge [11]. The average change in magnitude of CIV is approximately 6.5 kV for the ageing time duration of 1000 h and 4.2 kV at different ageing temperatures, at different gap distances. This attributes to 53.2% and 34% reduction in CIV due to ageing time and temperature respectively. Δ CIVavg is approximately 5.6 kV between the minimum and maximum gap distance for both ageing time and temperature.

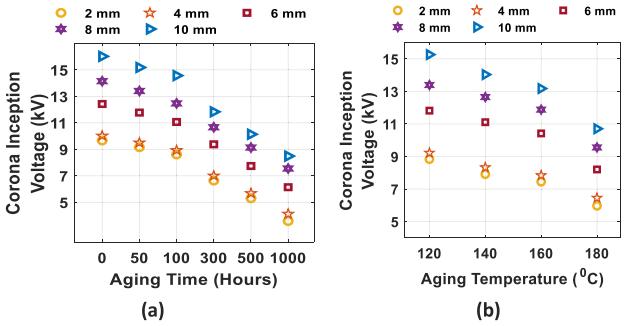

FIGURE 2. Effect of thermal ageing on CIV without the magnetic field for (a) Different ageing periods and (b) Different ageing temperatures.

Fig. 3(a) shows the variation of CIV with thermal ageing due to different ageing times by changing needle plane gap distance in presence of magnetic field as measured by UHF sensor. Fig. 3(b) shows the variation of CIV with thermal ageing due to different ageing temperatures by changing needle plane gap distance in presence of the magnetic field. A uniform magnetic field is applied by placing the test cell symmetrically between two permanent magnets. The resulting electromagnetic field produces Lorentz force which acts on the point charges produced near the needle tip. On comparing Fig. 3(a) and Fig. 3(b) decrease in the magnitude of CIV for corresponding ageing time and ageing temperature at all gap distances is observed. Due to the Lorentz force, all the charges move in the unified direction following a circular trajectory. The directed flow of electrons unlike the randomly moving electrons in absence of a magnetic field causes corona inception to take place at lower voltages. 54.3% reduction of CIV is observed in the thermally aged ester fluid with time in presence of the magnetic field. 39.4 % reduction of CIV is observed due to ageing temperature, in presence of the magnetic field. However, nearly 12.54%, 15.3 % and 19.7% reduction in CIV are observed due to magnetic field at fixed gap distance of 6 mm for unaged sample, 1000 h aged sample at 160°C and with 180°C aged for 250 hrs aged sample respectively. This reduction is marginal as compared to the reduction observed with the punga oil [14].

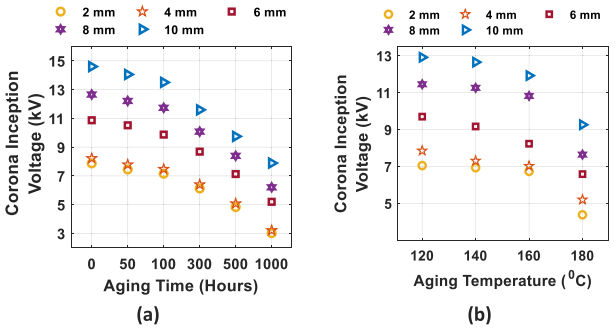

FIGURE 3. Effect of thermal ageing on CIV in the presence of magnetic field for (a) Different ageing periods (at 160°C) and (b) Different ageing temperatures.

2) SIGNAL ANALYSIS

Fig. 4(a) shows the time domain analysis of the typical UHF signal of an unaged sample with and without a magnetic field. The time plot of the UHF signal shows the intensity of UHF peaks decreases without the effect of the magnetic field. The width of the signal defined as the time when the signal magnitude lies between 20% of maximum value also shows a decrease in presence of the magnetic field. The width of the UHF signal is around 12.5 ns without a magnetic field and reduces to approximately 9 ns in presence of the magnetic field.

Fig. 4(b) shows the FFT analysis of the UHF signal acquired for unaged samples with and without a magnetic field. The frequency response curve shows the clear shift in the dominant peak of UHF signals with the magnetic field. While the dominant peak of the UHF signal is around 0.9 GHz in absence of a magnetic field, it is observed to be around 0.6 GHz in presence of the magnetic field. Also, it is to be noted that time and frequency domain analysis of acquired UHF signal for aged samples exhibited no significant change. Fig. 5 shows a hysteresis plot obtained at 6 mm gap distance

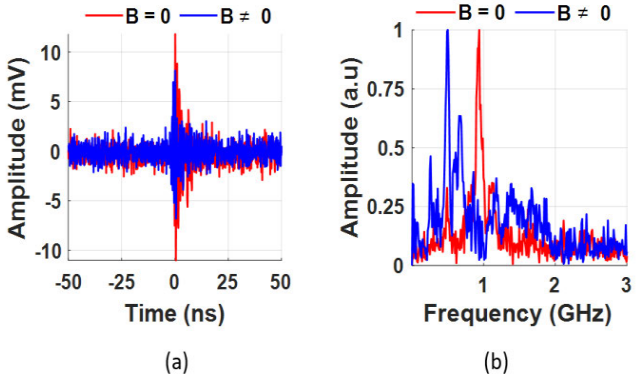

FIGURE 4. (a) Typical UHF signal (b) Fast Fourier transformer (FFT) analysis generated due to corona discharge activity in ester fluid in presence of the magnetic field.

for thermally aged ester fluid, at different applied voltage magnitudes. The hysteresis curve is plotted between applied voltage and peak magnitude of the UHF signal. To obtain the hysteresis plot, the CIV of the test sample is obtained and the output UHF signal is captured in sequence mode. Then the voltage is increased in steps of 200 V nearly up to 2 kV beyond CIV to trace the forward path of the hysteresis loop. To trace the reverse path, the output UHF signal is captured at the same voltage values which are used for tracing the forward path. The voltage is decreased beyond the inception point and the loop terminates at a value where corona extinction takes place. Each point in the loop corresponds to an average of peak-to-peak values of 100 sequences of UHF signal captured at a particular voltage. It is important to note that the magnitude of UHF peaks in the backward direction is greater than in the forward path because of remnant charges and hence corona extinction voltage (CEV) is less than CIV. Fig. 5 shows that CIV decreases with the increase in thermal ageing duration and temperature but the magnitude of UHF peaks increase with ageing. Hysteresis curve of 1000 h aged sample along with fluid samples thermally aged at 180°C has high magnitude UHF signal. The width of the hysteresis curve is found to increase with ageing which can be attributed to the significant increase in charges with ageing.

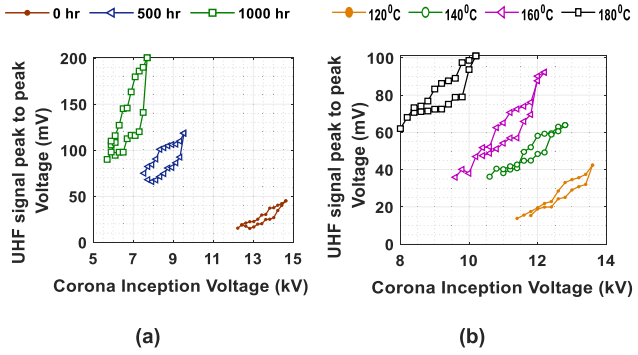

FIGURE 5. Hysteresis plot obtained with the thermally aged ester fluid (a) ageing times and (b) temperature at fixed gap distance.

Hysteresis plots follow the same trend in presence of a magnetic field as well as shown in Fig. 6(a) and (b). However, in presence of magnetic field hysteresis curve of each sample shows that both CIV and CEV are lesser in magnitude when compared with values in absence of magnetic field. Corresponding UHF peak magnitude is also found to be smaller in presence of the magnetic field. The magnetic field affects the trajectory of electrons which results in a possible decrease in magnitude and shape of the discharge plot. However, the width of the hysteresis curve does not follow any trend.

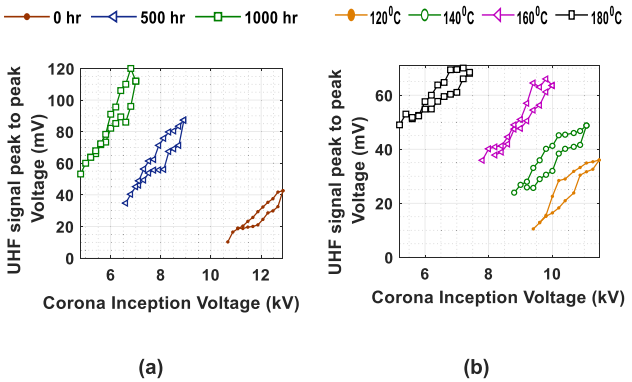

FIGURE 6. Hysteresis plot obtained with the thermally aged ester fluid in presence of magnetic field for (a) ageing times and (b) temperature at a fixed gap distance.

3) STATISTICAL ANALYSIS

The statistical analysis of the CIV data was carried out using Weibull and normal probability distribution plots. Marin and Wang, have clearly indicated, a detailed analysis is required to obtain the type of parametric distribution [27]. In the present study, initially hypothesis testing is carried out to check the type of distribution that experimental data follows. Shapiro–Wilk test is performed to check whether the data is normally distributed. So null hypothesis of the test is that experimental data follows the normal distribution. The value of confidence interval is chosen 95% and the significance level α is 5%. If p values are less than α then the hypothesis is rejected i.e. data does not follow the normal distribution. Therefore, when p> α data follows normal distribution [28]. Weibull distribution is defined by the equation:

$$f\,(V, \alpha, \beta) = 1 - \exp\left\{-\left(\frac{V}{\alpha}\right)^{\beta}\right\} \qquad (1)\ [27]$$

where V is the measured variable (CIV), f(V) is the probability of failure at a voltage, α is the scale parameter and is positive, and represents 63.2% probability of CIV occurrence, β is the shape parameter and is positive. On linearization, we obtain:

$$ln\left\{\frac{ln\,1}{[1 - f\,(V)]}\right\} = \beta(\ln V) - \beta.ln\,\alpha \qquad (2)\ [27]$$

Fig. 7(a) and Fig. 7(b) shows the Weibull probability plots for analysis of CIV without the magnetic field for different

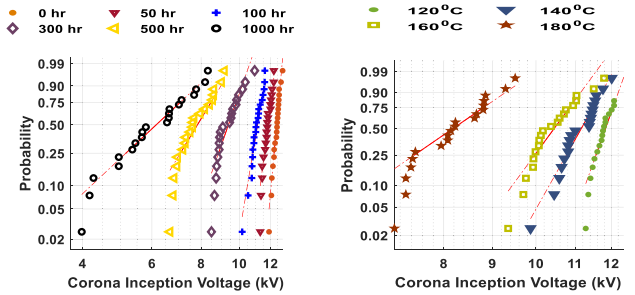

FIGURE 7. Weibull probability plots of thermally aged samples without magnetic field (a) fixed temperature (b) fixed ageing time.

TABLE 1. Parameters of weibull probability plot without magnetic field.

Ageing at 160°C	Linear fit equation	β	Ageing at 250 h	Linear fit equation	β
00 h	4.75x-59.55	4.75	120°C	3.23x-38.72	3.23
50 h	3.56x-42.56	3.56	140°C	2.23x-25.41	2.23
100 h	2.92x-32.99	2.92	160°C	1.77x-19.01	1.77
300 h	1.56x-15.19	1.56	180°C	1.14x-9.79	1.14
500 h	1.11x-9.22	1.11	-	-	-
1000 h	0.84x-5.87	0.84	-	-	-

ageing times and different ageing temperature respectively. The parameters of the Weibull plots are shown in Table 1.

The shape parameter β is a measure of the range of the CIV. β value around 3 indicates the normally distributed data and deviation from this value indicates the skewness. Table 1 shows that β decreases with an increase in thermal ageing. Larger values of β indicate that the scatter in the data is less and it can be observed that the unaged sample has the least scattered data and dispersion in data increases with ageing (both for fixed temperature and fixed time). The smaller deviation in CIV values in absence of the magnetic field can also be observed from the probability plot. Fig. 8(a) and (b) shows the Weibull probability plots for analysis of CIV with

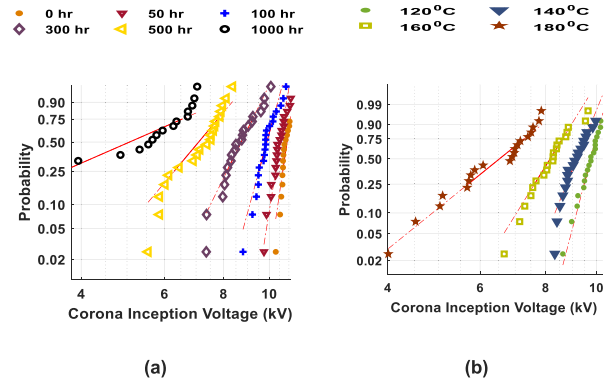

FIGURE 8. Weibull probability plots of thermally aged samples with magnetic field (a) fixed temperature (b) fixed ageing time.

TABLE 2. Parameters of weibull probability plot with magnetic field.

Ageing at 160°C	Linear fit equation	β	Ageing at 250 h	Linear fit equation	β
00 h	3.89x-42.92	3.89	120°C	3.16x-31.38	3.16
50 h	3.69x-39.46	3.69	140°C	2.09x-20.93	2.09
100 h	2.32x-23.42	2.32	160°C	1.58x-13.53	1.58
300 h	1.45x-13.22	1.45	180°C	1.12x-7.98	1.12
500 h	1.07x-8.14	1.07	-	-	-
1000 h	0.62x-3.45	0.62	-	-	-

magnetic field for different ageing times and different ageing temperature respectively. The parameters of the Weibull plots in the presence of the magnetic field are shown in Table 2.

β value again decreases with ageing in presence of the magnetic field. For the unaged sample, the β value is approximately the same with and without magnetic field but for corresponding ageing time and temperature β value is smaller when compared in absence of the magnetic field. Hence CIV data is more dispersed in the case of thermally aged samples when tested in presence of the magnetic field. It is because the insulation strength of fluid decreases with ageing and hence the effect of the magnetic field is more pronounced on aged samples as compared to unaged samples. Fig. 9 and Fig. 10 shows the normal distribution curves of CIV of different test

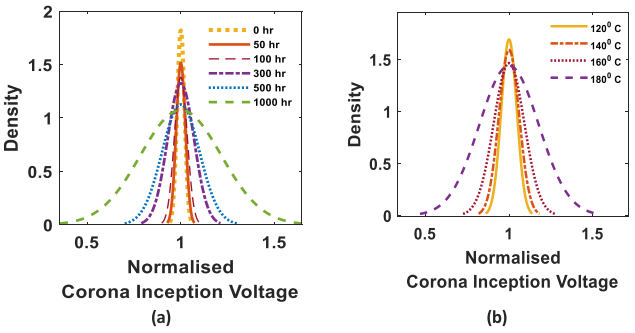

FIGURE 9. Normal distribution curves of CIV of thermally aged samples without magnetic field at (a) fixed temperature (160°C), (b) fixed ageing time (250 h).

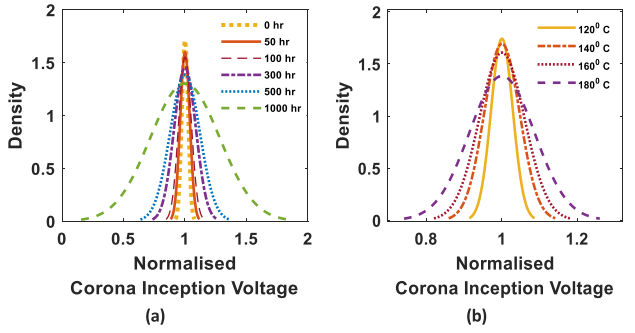

FIGURE 10. Normal distribution curves of CIV of thermally aged samples with the magnetic field at (a) fixed temperature (160°C), (b) fixed ageing time (250 h).

samples with and without magnetic field. The bell-shaped curves are normalised for the mean values of each test sample.

Irrespective of the effect of the magnetic field, distribution curves of unaged samples are sharply peaked indicating that most of the data is concentrated around the mean. This indicates that for unaged samples scatter in CIV data is less which is in coordination with the conclusion obtained from Weibull studies. However, with an increase in ageing time and temperature curves tend to become flat indicating the data spread farther from the mean value. In the absence of the magnetic field, deviation in data slightly increases and peakiness of the distribution curve starts decreasing with increasing ageing time and temperature. In presence of the magnetic field similar trend is observed with ageing time and temperature. The variation is on the higher side which can be explicitly observed as the bell curve shows leptokurtic nature for varying lesser ageing time and temperatures. The bell curve becomes mesokurtic when it is aged for a longer duration and at higher temperatures.

B. FLUORESCENT SPECTROSCOPIC STUDY OF THERMALLY AGED SYNTHETIC ESTER

Fluorescent spectroscopy is a relatively fast and sensitive method for the characterization and classification of different fluid samples. In fluorescence measurement, fluorescence intensity is plotted as a function of excitation wavelength [29]. Fig. 11 shows the fluorescent spectra of different synthetic ester fluid samples at different ageing times and ageing temperatures. The wavelength of 350 nm is used to excite the fluorescence spectra of synthetic ester fluid. A progressive shift in fluorescence maxima is observed with increasing ageing time and temperature. The inherent fluorophores in synthetic ester are the cause for fluorescence maxima of unaged fluid. With ageing, the insulating liquid starts degrading and the carbon particles start accumulating. This may be related to the decreased intensity of fluorescence with ageing. Further new decay products may form new chromophoric components due to which progressive redshift is being observed [30].

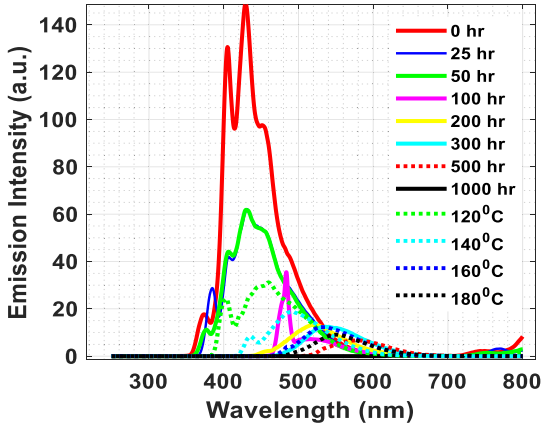

FIGURE 11. Fluorescent spectra of synthetic ester fluid.

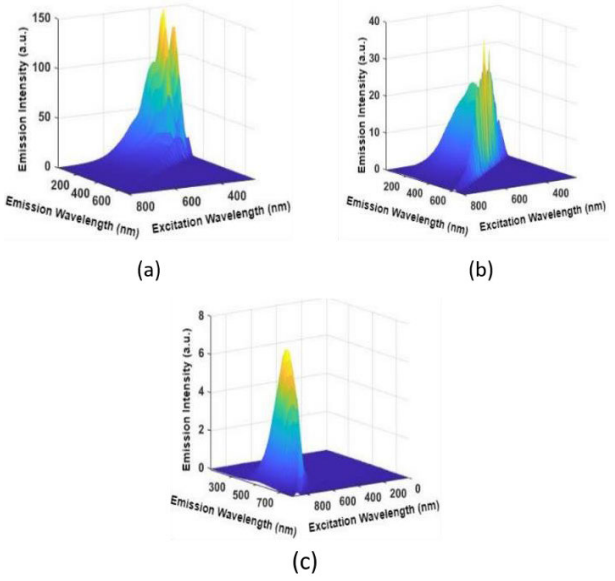

FIGURE 12. Excitation emission spectra of synthetic ester fluid samples.

The fluorescence spectral profile of insulating liquid samples can be better understood using 3-dimensional Excitation Emission Matrix (EEM) as shown in Fig. 12. It gives the correlation between excitation wavelength, emission wavelength and fluorescent intensity of test sample.

Fig. 12(a) shows that fluorescence emission for unaged fluid takes place for a range of 200-300 nm and has excitation spectra ranging between 250-450 nm. The fluorescence excitation maximum is found to be around 429 nm. Further, a redshift is observed in excitation and emission spectra along with reduced emission intensity for aged samples. Fig. 12(b) and Fig. 12(c) show redshift and reduction in emission intensity for 100h/160°C and 500h/160°C respectively. Hence, the changes in fluorescent spectral profile for thermal ageing can prove to be significant in determining the quality of the liquid in quick time.

C. DIELECTRIC LOSS ANALYSIS OF THERMALLY AGED SYNTHETIC ESTER

Dielectric loss is measured in terms of tan delta (dissipation factor) which is the measurement of the leakage current through the liquid. This leakage current is in turn a measure of the deterioration of the fluid. The insulating liquid is non-polar and deterioration results in polarization. Thus, the inability of insulating fluid to reorient itself at the molecular level results in dielectric loss [31]. This inability is temperature-dependent and governed by the molecular size, polarity and frequency of the alternating field. The dielectric response depends upon on enabling of dipole action and gives the measure of dissipation factor and permittivity of insulating liquid, as shown in equation 3:

$$tan\ \delta = \frac{\varepsilon'}{\varepsilon''} \quad (3)\ [32]$$

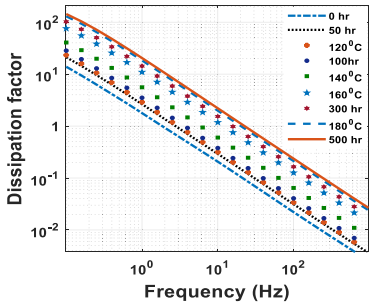

FIGURE 13. Variation in dielectric loss of thermally aged ester fluids at 90°C.

TABLE 3. Variation of dissipation factor at 50 hz at 90°C.

Sample	tan δ	Sample	tan δ
0 h	0.043	-	-
50 h	0.065	120°C	0.071
100 h	0.079	140°C	0.125
300 h	0.321	160°C	0.301
500 h	0.461	180°C	0.423
1000 h	3.292	-	-

where ε' is the real part of complex permittivity and ε'' is the complex part of complex permittivity. Dielectric response spectroscopy of synthetic ester fluid samples was carried out using OMICRON-DIRANA unit. All measurements were carried out at 50 Hz and different temperatures. Fig. 13 shows the variation of dissipation factor with frequency at different temperatures.

It can be observed that the dissipation factor shows proportional relation with age and an inverse relation with frequency. Higher dissipation factors indicate the polarization of liquid molecules due to thermal degradation. The exponential change in loss tangent with thermal degradation is also evident from test results of dielectric response at all temperatures. The inverse dielectric response of liquid samples with frequency is due to the hopping of charge carriers at low frequency resulting in low-frequency dispersion. The values of dissipation factor and electrical permittivity of different liquid samples at 50 Hz, 90°C are summarized as in Table 3. It can be seen that at 90°C loss tangent increases 82 times when the synthetic ester is aged for 1000 h and it increases more than 9 times when aged at 180°C for 250h.

D. FUZZY MODEL FOR DETECTION OF INSULATION CONDITION OF THERMALLY AGED SYNTHETIC ESTER

Automated condition monitoring of transformers is made possible by the application of artificial intelligence techniques. Condition monitoring involves the human thought processes so inherent uncertainty is always associated with the model [33]. Fuzzy logic manifests this vagueness and is hence one of the most widely used AI techniques in transformer monitoring [34]. In this work, fuzzy logic is used to correlate the spectral data with the dielectric spectroscopy results which indirectly indicates the condition of transformer insulation. The proposed fuzzy model is a two-input and single output Mamdani-type fuzzy inference system (FIS). The input spectral data for different aged samples of synthetic ester are not found to be precise since an overlap exists between two different samples. Fuzzy logic overcomes this problem of crisp threshold and facilitates the expression of the observed relationship of spectral data with ageing period and temperature in the form of minimal rules. Ageing period and temperature are indirectly related to insulation condition vis-a-vis corresponding dissipation factor. The construction of the fuzzy model is given as:

TABLE 4. Details of membership functions of input variables.

Redshift (nm)		Fluorescence intensity ratio	
Name	Crisp range	Name	Crisp range
RS_1	0-2	I_1	0-1
RS_2	2-51.5	I_2	1-2.4
RS_3	51.5-106	I_3	2.4-4.05
RS_4	106-149	I_4	4.05-12.06
RS_5	>149	I_5	12.06-22.38
		I_6	>22.38

TABLE 5. Rule base for detecting insulation condition.

If FIR is I_1 then insulation is **healthy**
If FIR is I_2 and redshift is RS_1 then insulation is **healthy**
If FIR is I_2 and redshift is RS_2 then insulation is **healthy**
If FIR is I_3 and redshift is RS_2 then insulation is **healthy**
If FIR is I_4 and redshift is RS_3 then insulation is **healthy**
If FIR is I_5 and redshift is RS_3 then insulation is **deteriorating**
If FIR is I_5 and redshift is RS_4 then insulation is **deteriorating**
If FIR is I_6 and redshift is RS_5 then insulation has reached the **end of life**

1) INPUT AND OUTPUT VARIABLES

The different input and output variables used for the fuzzy model are indicated below:

(i) Redshift: The shift in excitation wavelength corresponding to fluorescence maxima of different aged samples for virgin liquid is known as the redshift. This shift in the fluorescence maxima is taken as one of the input variables of FIS. The fuzzification of input space is carried out using six membership functions defined by (S1 –S5) which convert crisp values of redshift for each aged sample into linguistic expression.

(ii) Fluorescence intensity ratio: The ratio of fluorescence intensity of virgin fluid to intensity of the aged sample is used as another input variable to the developed FIS. This variable is fuzzified using seven membership functions I1 to I7.

(iii) Insulation condition: Redshift and intensity ratio of the fluorescent spectrum are mapped to insulation condition in the developed FIS. The correlation is obtained from the

TABLE 6. Testing of fuzzy model.

Sample	(nm)	a.u.	Input (RS, I)	Defuzzied output	Predicted Insulation condition	Dissipation factor	Expected Insulation condition
25h/160°C	430	62.2	1,2.39	0.5	Healthy	0.051	Healthy
75h/160°C	450.7	49.38	21.7,1.87	0.5	Healthy	0.067	Healthy
250h/130°C	488	24	59,6.21	0.5	Healthy	0.107	Healthy
250h/150°C	522.7	13.09	93.7,11.38	0.5	Healthy	0.219	Healthy
250h/170°C	542.8	11.03	113.8,13.5	1.5	Deteriorating	0.396	Deteriorating

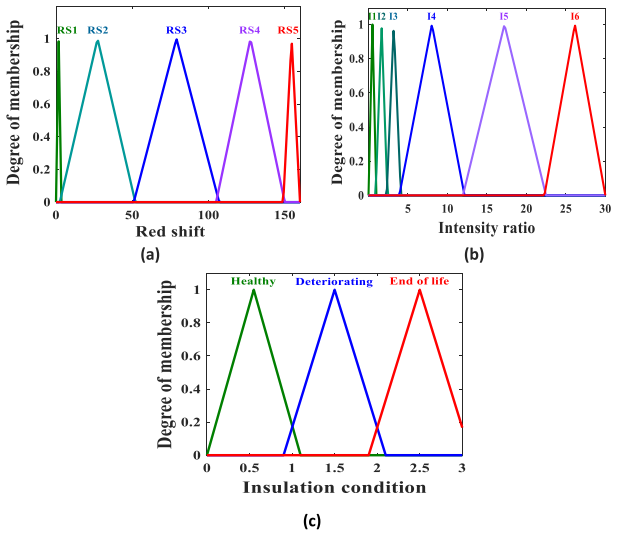

FIGURE 14. (a) Membership function plot for redshift, (b) Membership function plot for Fluorescence intensity ratio, (c) Membership function plot for insulation condition.

dielectric spectroscopy response of the thermally degraded synthetic ester samples. The dissipation factor of synthetic ester fluid is measured which helps us to identify the insulation condition as pec IEC 61099. Hence insulation condition is taken as the output variable of FIS. The fuzzification of output space is carried out using three membership functions defined by linguistic variables healthy insulation ($\tan\delta < 0.3$), deteriorating insulation ($0.3 < \tan\delta < 3$) and end of life ($\tan\delta > 3$) [37].

The pictorial representation of the membership function of input and output variables is given in Fig. 14 and details are given in Table 4.

2) FORMULATION OF RULE BASE

The input-output mapping of the FIS is defined by eight expert rules. The redshift along with the fluorescence intensity ratio defines the extent of thermal degradation. The dissipation factor obtained from dielectric spectroscopy analysis of thermally degraded samples is indicative of the insulation condition. Hence, a rule base is formulated using dielectric spectroscopy results in such a way that for the ageing time of up to 250 h and ageing temperature up to 160°C, insulation is considered healthy. If ageing time or temperature exceeds 250 h and 160°C respectively, insulation starts deteriorating. However, if insulation ageing time reaches 1000 h for 160°C and beyond, insulation is severely degraded and immediate replacement is required. These rules are further backed by CIV values obtained during the electrical characterization of the aged samples. The rules defined for the proposed FIS are given in Table 5.

Since both redshift and fluorescence intensity ratio are used as inputs, AND operator is used for implication. All rules are given an equal weightage of 1 and the aggregation operator is OR. If the insulation condition is healthy then the transformer is said to be in an acceptable state and no specific action is required. When insulation condition is deteriorating then regular monitoring is required. If insulation condition indicates the end of life, then urgent replacement of transformer insulation is required.

3) TESTING AND VALIDATION OF MODEL

In this work, analysis of thermally aged synthetic ester fluid is carried out using 10 samples. Out of these, 6 samples are aged for different times at the fixed temperature of 160°C and the remaining 4 are aged at different temperatures for the fixed time corresponding to 250 h. A fuzzy model for detecting the condition of synthetic ester when used as an insulating fluid in transformers is constructed using spectral data of 10 samples. For testing and validation of the model, 5 new samples are prepared. The details of these samples are given in Table 6. Fig. 11 shows that test sample 160°C/25h has fluorescence peak at 430 nm and emission intensity of 62 a.u. This corresponds to a redshift of 0.5 nm and a fluorescence intensity ratio of 2.29. Using (0.5, 2.29) as inputs, the fuzzy model gives the defuzzified value of 0.5 as rule 2 is satisfied which indicates deteriorating insulation. This is validated by dielectric spectroscopy results of the sample showing a dissipation factor of 0.051 which is indicative of healthy insulation. Similarly, test sample 170°C/250h has a fluorescence peak at 542.8 nm and emission intensity of 11.03 a.u. This corresponds to a redshift of 113.3 nm and a fluorescence intensity ratio of 13.5. Using (113.3, 13.5) as inputs, the fuzzy model gives the defuzzified value of 1.5 as rule 7 is satisfied which indicates unhealthy insulation. This is validated by dielectric spectroscopy results of the sample showing dielectric loss of 0.396 which is indicative of deteriorating insulation condition.

III. CONCLUSION

The main conclusions of the reported work are summarized as under:

- CIV measurement studies were carried out with thermally aged ester fluid, in presence of the magnetic field. 54.3% reduction in CIV is observed with the thermally aged ester fluid in presence of the magnetic field. It is realised that ageing temperature and time have a high influence on the reduction of CIV, in presence of a magnetic field.
- The FFT analysis of the UHF signal obtained due to corona activity, in presence of a magnetic field, shows a shift in dominant frequency towards the lower frequency range. The UHF signal magnitude formed due to corona activity at different voltages forms a hysteresis loop. However, the width of the hysteresis loop increases with ageing but it is not influenced by the magnetic field.
- Statistical analysis is carried out with corona inception voltage using Weibull distribution studies both in the presence and absence of a magnetic field. The shape parameter β decreases with an increase in ageing time and temperature. Based on the analysis, it is realised that the scatter in data is high in presence of the magnetic field.
- Fluorescent spectroscopy of thermally aged samples shows the progressive redshift along with decreased fluorescence intensity. This sensitive and less time-consuming technology can serve as a potential diagnostic tool for monitoring the liquid insulation condition of transformers. Dielectric spectroscopy study shows an increase in values of dissipation factor of thermally aged synthetic ester fluid.
- To automate the transformer condition monitoring scheme, a fuzzy model is constructed to correlate the performance analysis of thermally aged synthetic ester fluid using these characterizations and predict the status on the end life of the insulation. This model accounts for thermal ageing due to both ageing time and temperature, which is unique.

Synthetic ester fluid being a renewable substitute of mineral oil, further studies need to be carried out to explore its usability as a transformer insulant. In future work, other optical techniques like less cost-intensive and technically simpler PL spectroscopy will be used for analysing the performance of synthetic ester. AI-based health index model to assess the condition of this insulant with ageing can be developed as a part of the condition monitoring scheme.

REFERENCES

[1] L. J. Zhou, G. N. Wu, and J. Liu, "Modeling of transient moisture equilibrium in oil-paper insulation," *IEEE Trans. Dielectr. Electr. Insul.*, vol. 15, no. 3, pp. 872–878, Jun. 2008.

[2] P. Kurzweil, C. Schell, R. Haller, P. Trnka, and J. Hornak, "Environmental impact and aging properties of natural and synthetic transformer oils under electrical stress conditions," *Adv. Sustain. Syst.*, vol. 5, no. 8, Aug. 2021, Art. no. 2100079.

[3] P. Trnka, J. Hornak, P. Prosr, O. Michal, and F. Wang, "Various aging processes in a paper-natural ester insulation system in the presence of copper and moisture," *IEEE Access*, vol. 8, pp. 61989–61998, 2020.

[4] T. Wan, H. Qian, Z. Zhou, S. K. Gong, X. Hu, and B. Feng, "Suppressive mechanism of the passivator Irgamet 39 on the corrosion of copper conductors in transformers," *IEEE Trans. Dielectr. Electr. Insul.*, vol. 19, no. 2, pp. 454–459, Apr. 2012.

[5] S. Singha, R. Asano, G. Frimpong, C. C. Claiborne, and D. Cherry, "Comparative aging characteristics between a high oleic natural ester dielectric liquid and mineral oil," *IEEE Trans. Dielectr. Electr. Insul.*, vol. 21, no. 1, pp. 149–158, Feb. 2014.

[6] P. Przybylek, K. Walczak, W. Sikorski, H. Moscicka-Grzesiak, H. Moranda, and M. Cybulski, "Experimental validation of a method of drying cellulose insulation in distribution transformers using circulating synthetic ester," *IEEE Access*, vol. 9, pp. 150322–150329, 2021.

[7] J. Hao, M. Dan, R. Liao, and J. Li, "Effect of moisture on particles accumulation and oil breakdown characteristics in mineral oil and natural ester under non-uniform DC electrical field," *IEEE Access*, vol. 7, pp. 101785–101794, 2019.

[8] S. A. Ward, A. El-Faraskoury, M. Badawi, S. A. Ibrahim, K. Mahmoud, M. Lehtonen, and M. M. Darwish, "Towards precise interpretation of oil transformers via novel combined techniques based on DGA and partial discharge sensors," *Sensors*, vol. 21, no. 6, pp. 1–21, 2021.

[9] N. Izeki, A. Kurahashi, and K. Matsuura, "Behavior of oil corona and damage of transformer insulation," *IEEE Trans. Power App. Syst.*, vol. PAS-90, no. 5, pp. 2330–2338, Sep. 1971.

[10] M. A. Abouelatta, S. A. Ward, A. M. Sayed, K. Mahmoud, M. Lehtonen, and M. M. F. Darwish, "Fast corona discharge assessment using FDM integrated with full multigrid method in HVDC transmission lines considering wind impact," *IEEE Access*, vol. 8, pp. 225872–225883, 2020.

[11] A. J. Amalanathan, R. Sarathi, S. Prakash, A. K. Mishra, R. Gautam, and R. Vinu, "Investigation on thermally aged natural ester oil for real-time monitoring and analysis of transformer insulation," *High Voltage*, vol. 5, no. 2, pp. 209–217, Apr. 2020.

[12] A. Bhangaonkar, S. Kulkarni, and R. Shevgaonkar, "Study of the effects of alternating magnetic field on point-plane corona," *IEEE Trans. Dielectr. Electr. Insul.*, vol. 18, no. 6, pp. 1813–1820, Dec. 2011.

[13] D. M. Hepburn, B. G. Steward, L. A. Dissado, and J. C. Fothergill, "Magnetic field disturbance of partial discharge activity in a cone-plane gap," in *Proc. Electr. Insul. Conf. Electr. Manuf. Expo.*, Oct. 2007, pp. 142–145.

[14] S. Murugesan, A. J. Amalanathan, R. Sarathi, B. Srinivasan, and R. Samikannu, "Investigation on impact of magnetic field on the corona discharge activity in Punga oil using fluorescent fiber and UHF sensor techniques," *IEEE Access*, vol. 9, pp. 129218–129228, 2021.

[15] M. R. Hussain, S. S. Refaat, and H. Abu-Rub, "Overview and partial discharge analysis of power transformers: A literature review," *IEEE Access*, vol. 9, pp. 64587–64605, 2021.

[16] P. Przybylek and J. Gielniak, "Analysis of gas generated in mineral oil, synthetic ester, and natural ester as a consequence of thermal faults," *IEEE Access*, vol. 7, pp. 65040–65051, 2019.

[17] Y. Wang, H. Yuan, X. Liu, Q. Bai, H. Zhang, Y. Gao, and B. Jin, "A comprehensive study of optical fiber acoustic sensing," *IEEE Access*, vol. 7, pp. 85821–85837, 2019.

[18] S. Thakur, R. Sarathi, and M. G. Danikas, "Investigation on thermal ageing impact on dielectric properties of natural ester oil," *Electr. Eng.*, vol. 101, no. 3, pp. 1007–1018, Sep. 2019.

[19] N. A. Bakar and A. Abu-Siada, "A new method to detect dissolved gases in transformer oil using NIR-IR spectroscopy," *IEEE Trans. Dielectr. Electr. Insul.*, vol. 24, no. 1, pp. 409–419, Feb. 2017.

[20] A. M. Alshehawy, D.-E.-A. Mansour, M. Ghali, M. Lehtonen, and M. M. F. Darwish, "Photoluminescence spectroscopy measurements for effective condition assessment of transformer insulating oil," *Processes*, vol. 9, no. 5, p. 732, Apr. 2021.

[21] B. Wicaksono, H. Kong, L. V. Markova, and H.-G. Han, "Application of fluorescence emission ratio technique for transformer oil monitoring," *Measurement*, vol. 46, no. 10, pp. 4161–4165, Dec. 2013.

[22] M. Kozioł, Ł. Nagi, M. Kunicki, and I. Urbaniec, "Radiation in the optical and UHF range emitted by partial discharges," *Energies*, vol. 12, no. 22, p. 4334, Nov. 2019.

[23] X. Wu, Z. Zhao, R. Tian, S. Gao, Y. Niu, and H. Liu, "Exploration of total synchronous fluorescence spectroscopy combined with pre-trained convolutional neural network in the identification and quantification of vegetable oil," *Food Chem.*, vol. 335, Jan. 2021, Art. no. 127640.

[24] M. Elsisi, M. Tran, K. Mahmoud, D.-E.-A. Mansour, M. Lehtonen, and M. M. F. Darwish, "Effective IoT-based deep learning platform for online fault diagnosis of power transformers against cyberattacks and data uncertainties," *Measurement*, vol. 190, Feb. 2022, Art. no. 110686.
[25] L. J. Yang, W. Sun, S. Gao, and J. Hao, "Thermal aging test for transformer oil–paper insulation under over-load condition temperature," *IET Gener., Transmiss. Distrib.*, vol. 12, no. 12, pp. 2846–2853, Jul. 2018.
[26] C. G. Azcarraga, A. Cavallini, and U. Piovan, "A comparison of the voltage withstand properties of ester and mineral oils," *IEEE Elect. Insul. Mag.*, vol. 30, no. 5, pp. 6–14, Sep. 2014.
[27] D. Martin and Z. Wang, "Statistical analysis of the AC breakdown voltages of ester based transformer oils," *IEEE Trans. Dielectrics Electr. Insul.*, vol. 15, no. 4, pp. 1044–1050, Aug. 2008.
[28] U. Khaled and A. Beroual, "AC dielectric strength of synthetic ester-based Fe_3O_4, Al_2O_3 and SiO_2 nanofluids—Conformity with normal and Weibull distributions," *IEEE Trans. Dielectr. Electr. Insul.*, vol. 26, no. 2, pp. 625–633, Apr. 2019.
[29] Y. Gilbert, H. Ghalila, M. B. Onana, Y. Majdi, Z. B. Lakhdar, H. Mezlini, and S. Sevestre-Ghalila, "Characterization of vegetable oils by fluorescence spectroscopy," *Food Nutr. Sci.*, vol. 2, no. 7, pp. 692–699, Sep. 2011.
[30] S. K. Panigrahi, S. Thakur, R. Sarathi, and A. K. Mishra, "Understanding the physico-chemical properties of thermally aged natural ester oil adopting fluorescent technique," *IEEE Trans. Dielectr. Electr. Insul.*, vol. 24, no. 6, pp. 3460–3470, Dec. 2017.
[31] W. Bassi and H. Tatizawa, "Conductivity and dielectric dissipation factor (tan δ) measurements of insulating oils of new and aged power transformers—Comparison of results between portable square wave and conventional bridge methods," *IEEE Elect. Insul. Mag.*, vol. 37, no. 5, pp. 14–25, Sep. 2021.
[32] S. S. M. Ghoneim, S. S. Dessouky, A. Boubakeur, A. A. Elfaraskoury, A. B. Abou Sharaf, K. Mahmoud, M. Lehtonen, and M. M. F. Darwish, "Accurate insulating oil breakdown voltage model associated with different barrier effects," *Processes*, vol. 9, no. 4, p. 657, Apr. 2021.
[33] Y.-C. Huang and H.-C. Sun, "Dissolved gas analysis of mineral oil for power transformer fault diagnosis using fuzzy logic," *IEEE Trans. Dielectr. Electr. Insul.*, vol. 20, no. 3, pp. 974–981, Jun. 2013.
[34] H. Malik, A. K. Yadav, S. Mishra, and T. Mehto, "Application of neuro-fuzzy scheme to investigate the winding insulation paper deterioration in oil-immersed power transformer," *Int. J. Electr. Power Energy Syst.*, vol. 53, pp. 256–271, Dec. 2013.
[35] A. E. B. Abu-Elanien, M. M. A. Salama, and M. Ibrahim, "Calculation of a health index for oil-immersed transformers rated under 69 kV using fuzzy logic," *IEEE Trans. Power Del.*, vol. 27, no. 4, pp. 2029–2036, Oct. 2012.

MRIDULA is currently a Research Scholar with the Department of Electrical Engineering, IIT Madras, Chennai, India. Her research interests include condition monitoring of HV equipment and transformer liquid insulation.

SHUFALI ASHRAF WANI received the B.Tech. degree from the University of Kashmir, India, in 2011, and the M.Tech. degree in instrumentation and control and the Ph. D. degree in electrical engineering from Jamia Millia Islamia (a Central University), New Delhi, India, in 2014 and 2019, respectively. She was an Assistant Professor (on contract) with the Department of Electrical Engineering, National Institute of Technology, Srinagar. She is currently a Postdoctoral Fellow with the Electrical Engineering Department, IIT Madras. Her research interests include dissolved gas analysis, application of intelligent techniques to electrical engineering problems, sensoars, and electronic instrumentation.

A. J. AMALANATHAN is currently a Research Scholar with the Department of Electrical Engineering, IIT Madras, Chennai, India. His research interest includes condition monitoring of ester and its nanofluids for power transformers.

R. SARATHI (Senior Member, IEEE) is currently a Professor and the Head of High Voltage Laboratory, Department of Electrical Engineering, IIT Madras, Chennai, India. His research interest includes condition monitoring of power apparatus and nanomaterials.